Plasmonics (2018) 13:555–561
DOI 10.1007/s11468-017-0543-z

Morphology Optimization of Silver Nanoparticles Used to Improve the Light Absorption in Thin-Film Silicon Solar Cells

Zhiqiang Duan[1,2] · **Meicheng Li**[2,3] · **Trevor Mwenya**[2] · **Yingfeng Li**[2] · **Dandan Song**[2]

Received: 28 November 2016 / Accepted: 9 February 2017 / Published online: 20 February 2017

Abstract Silver nanoparticle (NP) arrays are used as antireflection coating to enhance light trapping capability of thin-film silicon solar cells. In this paper, we theoretically investigate the differences of light absorption distribution between the silver NP (spherical and hemispherical) array layer and the crystalline silicon (CS) substrate. Compared to the naked silicon of the same thickness, the results show that only the flattened hemispherical silver NPs can really improve the light trapping ability and make the light absorption of CS body increase by 26%; the optimum ratio of lateral (NP diameter divided by the array periodicity) and longitudinal (NP height divided by diameter) are 0.86 and 0.22, respectively.

Keywords Antireflection coatings · Geometric optical design · Thin films · Nanomaterials

Introduction

Metal nanoparticle (NP) arrays can interact intensively with the incident sunlight and harvest it because they have surface plasmons. The captured energy carried by sunlight is confined to metal NP surfaces and used to increase the local temperature, generate hot electrons, and enhance localized electric field through different mechanisms [1, 2]. A lot of papers have investigated these mechanisms and applied them in NP-enhanced optoelectronic devices successfully [3, 4]. In thin-film solar cells, based on diffraction coupling of localized plasmons in which resonance occurs mostly in the visible or infrared region of the electromagnetic spectrum, metal NPs are also used as plasmonic antireflection coatings to increase the light absorption [5–7]. The optical properties of metal NPs are affected by their shape and size, the length of arrays, the dielectric constant of surrounding medium, and so on [8–11]. This article studies the optical properties of thin-film silicon solar cells from a different point of view, the difference of light absorption distribution between the antireflection coating and the crystalline silicon (CS) body.

In the experiment, the metal NP layer and thin-film substrate are considered as one whole body so as to discuss the optical properties, and the difference of light absorption distribution between them is not distinguishable. However, in theory, they can be discussed as two different parts separately. Therefore, this study is different from the previous ones in that it focuses and emphasizes on the distribution of absorbed photons in the two parts. As shown in Fig. 1a, the total light absorption (A) can be divided into two parts: $A = A_{Ag} + A_{Si}$. A_{Ag} is one part which has been absorbed by silver NP array layer and A_{Si} is the other part which has been absorbed by thin-film CS substrate. So, in order to get better and effective light absorption, there is need not only to reduce the light reflection (R) and transmission (T) but also to decrease the proportion of A_{Ag} in the total absorption, which can be easily seen from the formula $A_{Si} = 1 - R - T - A_{Ag}$.

Considering each absorbed photon with energy greater than the band gap produces one and only one electron-hole pair, for the purpose of quantitative comparison, compared to the naked CS with the same thickness, two enhancement

✉ Meicheng Li
mcli@ncepu.edu.cn

[1] School of Mathematical and Physical Science, North China Electric Power University, Beijing 102206, China

[2] State Key Laboratory of Alternate Electrical Power System with Renewable Energy Sources, School of Renewable Energy, North China Electric Power University, Beijing 102206, China

[3] Chongqing Materials Research Institute, Chongqing 400707, China

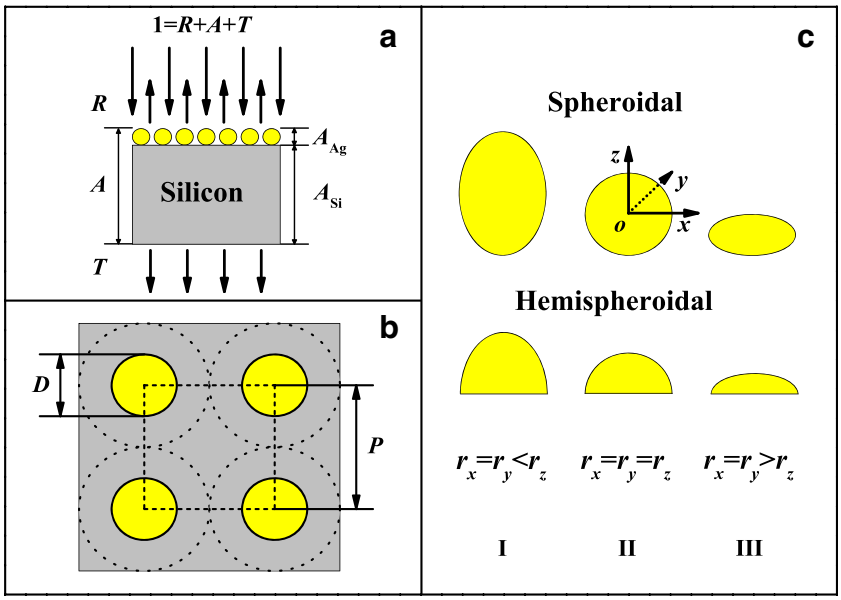

Fig. 1 **a** Distribution of light absorption (A_{Ag} and A_{Si} are light absorptions of silver NP antireflection layer and CS body, respectively). **b** Structure diagram of NP arrays (D is the NP diameter; P is the period length). **c** Different shapes of NPs with spheroidal and hemispheroidal (I, $r_x = r_y < r_z$; II, $r_x = r_y = r_z$; III, $r_x = r_y > r_z$)

factors of efficient light trapping E_T and effective light absorption E_A are defined as follows:

$$E_T = \frac{N_t - N_{nSi}}{N_{nSi}} \quad (1)$$

$$E_A = \frac{N_{Si} - N_{nSi}}{N_{nSi}} \quad (2)$$

here,

$$N_t = \int A(\lambda) F(\lambda) \lambda / (h_0 c_0) d\lambda \quad (3)$$

$$N_{Si} = \int A_{Si}(\lambda) F(\lambda) \lambda / (h_0 c_0) d\lambda \quad (4)$$

$$N_{nSi} = \int A_{nSi}(\lambda) F(\lambda) \lambda / (h_0 c_0) d\lambda \quad (5)$$

N_t is the total number of absorbed photons in the whole body including the CS substrate and metal NP antireflective coating. N_{Si} is the number of absorbed photons in the CS substrate which is a part of the whole, and N_{nSi} is the number of absorbed photons of the naked CS. $A(\lambda)$, $A_{Si}(\lambda)$, and $A_{nSi}(\lambda)$ are the corresponding light absorption coefficient. $F(\lambda)$ is the distribution of solar radiation spectral intensity on the Earth's surface under AM 1.5 spectrum [12]. λ is the wavelength of incident light; h_0 and c_0 are Planck constant and speed of light in vacuum, respectively. As shown in Fig. 1b, c, the metal NPs with the diameter of D are arranged in a square array with array length of P, and two shapes of NPs (spheroidal and hemispheroidal) with different sizes are taken into consideration.

Simulation Methods

In our theoretical calculations, the net radiation method [NRM] is used because it provides good matching between simulation and experimental results [13–15]. Moreover, it is very suitable for calculating the reflection, transmission, and absorption characteristics of each layer in a multilayer medium system. As shown in Fig. 2a, a system of M layers, I, III and II, IV represent the incoming and outgoing electromagnetic radiation fluxes (E), respectively. The interfaces are labeled j

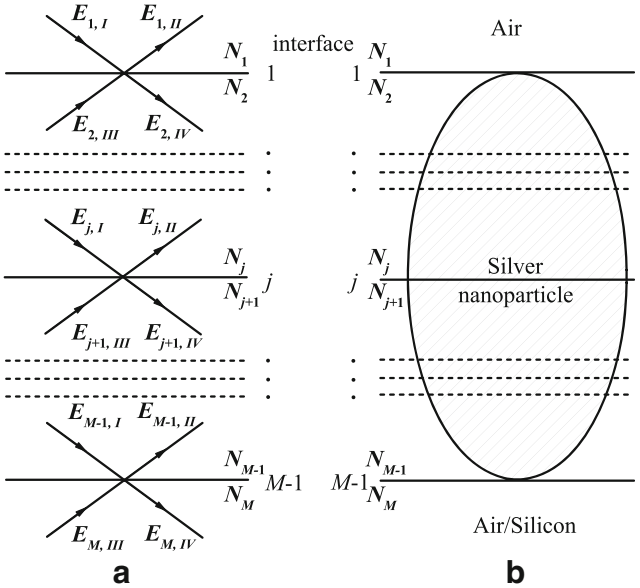

Fig. 2 **a** Schematic multilayer structure, with numbering convention of interfaces (1, …, j, …, $M-1$), complex refractive index (N_1, …, N_j, …, N_M), and electromagnetic radiation fluxes ($E_{j,I}$, $E_{j,II}$, $E_{j+1,III}$, $E_{j+1,IV}$, …). **b** Schematic representation of silver NP and effective multilayer structure

($j = 1, \cdots, M-1$) and the complex refractive index of j-th medium is N_j. For every interface j, there are four equations and the relations between the incoming and outgoing electromagnetic radiation fluxes can be expressed as follows:

$$\begin{cases} E_{j,I} = & \tau_j E_{j,IV} \\ E_{j,II} = r_{j,j+1}E_{j,I} + & t_{j+1,j}E_{j+1,III} \\ E_{j+1,III} = & \tau_{j+1}E_{j+1,II} \\ E_{j+1,IV} = t_{j,j+1}E_{j,I} + & r_{j+1,j}E_{j+1,III} \end{cases} \quad (6)$$

The reflection and transmission coefficient at each of the interface are $r_{j,j+1}$ and $t_{j,j+1}$ which are determined using Fresnel's laws; τ_j is the absorption attenuation rate of layer j, defined by

$$\tau_j = \exp\left(-\alpha d_j/\cos\varphi\right) \quad (7)$$

where $\alpha = 4\pi k_j/\lambda$ is the absorption coefficient and $d_j/\cos\varphi$ is the distance that electromagnetic radiation travels through the layer of thickness d_j with propagation angle φ. k_j is the imaginary part of the complex refractive index $N_j = n_j - ik_j$. Both the real refractive index n_j and the extinction coefficient k_j are functions of λ. Assuming the incident electromagnetic radiation flux $E_{1,I} = 1$ and $E_{M,III} = 0$, then, for each layer j, the spectral reflectance $R_j = E_{j-1,II}$, transmittance $T_j = E_{j+1,IV}$, and absorptance $A_j = E_{j,II} - E_{j,III} + E_{j,IV} - E_{j,I}$ can be worked out.

The effective multilayer structure of metal NPs is shown in Fig. 2b, and the complex dielectric constant of different NP layers can be solved by the effective medium approximation which is appropriate for combining both the metal particles and medium [16]:

$$\frac{\varepsilon_e - \varepsilon_0}{\varepsilon_e + 2\varepsilon_0} = f\frac{\varepsilon_{Ag} - \varepsilon_0}{\varepsilon_{Ag} + 2\varepsilon_0} \quad (8)$$

where f is the ratio of volume filling of metal NPs. ε_0, ε_{Ag}, and ε_e are the complex dielectric constants of air, silver [17], and the interlayer of silver NPs, respectively.

Before starting the calculations, related parameters are assumed as follows: the diameter of silver NPs can change from 0 to 200 nm which is also the maximum value of array length P and the thickness of CS substrate is 100 μm; the layer thickness $d_j = 1$ nm and it is also the minimum step in calculating.

Results and Discussion

Compared to the continuous silver film, silver NPs have very different optical properties and they depend on the NP shapes and sizes. Under the different parameters, the light reflectivity, absorptivity, and transmissivity of silver NPs surrounded by air are shown in Fig. 3. Figure 4 shows the results when silver NPs are used as antireflection coating on the CS substrate.

For the continuous silver film, there is an obvious characteristic absorption peak at the wavelength of 0.316 μm. Most of the light ($\lambda > 0.316$ μm) is fully reflected and the transmitted light is almost zero which are shown in Fig. 3. However,

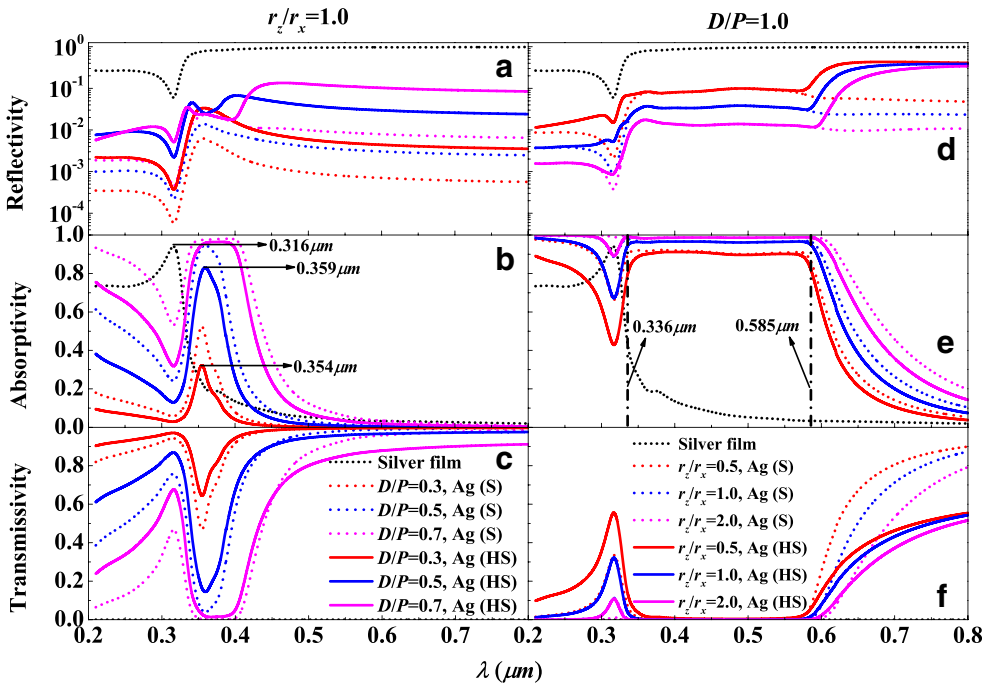

Fig. 3 Optical properties of silver NPs (spheroidal (S) and hemispheroidal (HS)) surrounded by air under different parameters compared to the silver film with a thickness of 100 nm. **a**, **b**, and **c** are the light reflectivity, absorptivity, and transmissivity of different ratios of D/P (0.3, 0.5, and 0.7) under $r_z/r_x = 1.0$, respectively. **d**, **e**, and **f** are the light reflectivity, absorptivity, and transmissivity of different ratios of r_z/r_x (0.5, 1.0, and 2.0) under $D/P = 1.0$, respectively

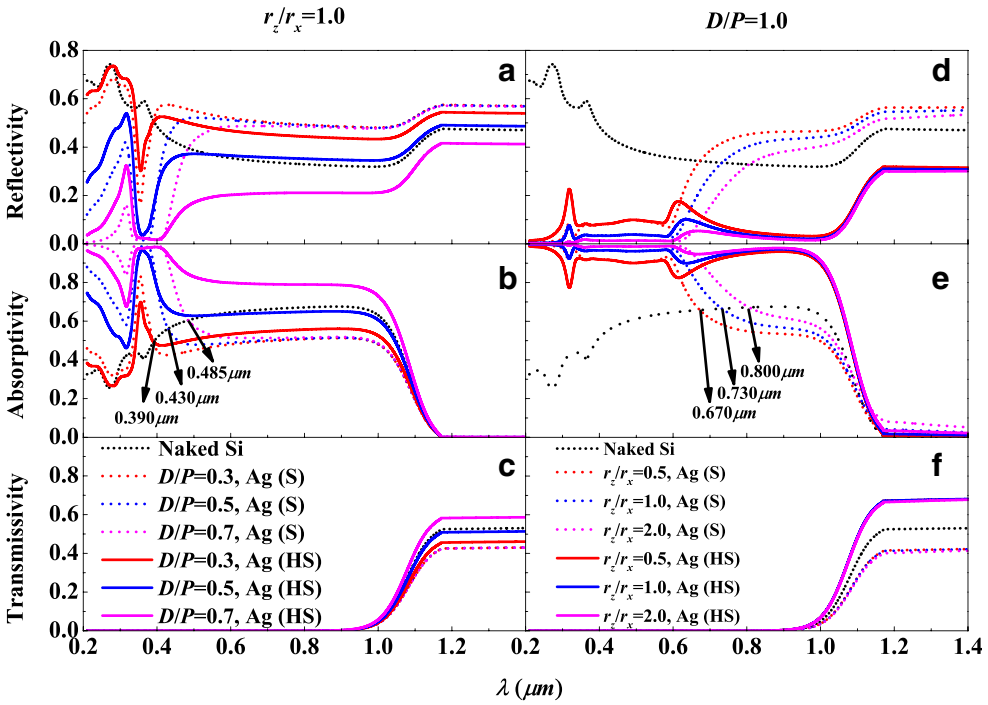

Fig. 4 Optical properties of CS with silver NPs (spheroidal (S) and hemispheroidal (HS)) as antireflection coating under different parameters compared to the naked silicon. **a**, **b**, and **c** are the light reflectivity, absorptivity, and transmissivity of different ratios of D/P (0.3, 0.5, and 0.7) under $r_z/r_x = 1.0$, respectively. **d**, **e**, and **f** are the light reflectivity, absorptivity, and transmissivity of different ratios of r_z/r_x (0.5, 1.0, and 2.0) under $D/P = 1.0$, respectively

for the discontinuous silver NPs, at the same wavelength, the absorption peak which occurred in the continuous silver film is reversed and changed into transmission peak [9, 18, 19]. Under $r_z/r_x = 1.0$, with increase in silver NP diameter, one or two peaks appear in the light reflection of the two shapes of NPs (Fig. 3a), and they have the trend to shift to long wavelength direction. The reflection is also stronger with the larger diameter especially at long wavelengths and the hemispheroidal NPs have larger light reflection than the spheroidal NPs. For the light absorption (Fig. 3b), both shapes of silver NPs form new absorption peaks at the same position and they are only correlated with the transverse diameter (The absorption peaks are at the wavelength of 0.354 μm for $D/P = 0.3$ and 0.359 μm for $D/P = 0.5$). Moreover, with the increase of transverse diameter, absorption intensity also increases and absorption peaks begin to gradually widen when $D/P \geq 0.6$, and eventually, they become flat which means there is strong light absorption. In addition, the spheroidal NPs have larger absorption than the hemispheroidal NPs because of the larger volume. This is shown in Fig. 3b, e. Under $D/P = 1.0$, as shown in Fig. 3d–f, different values of r_z mainly affect the intensity of the light absorption, reflection, and transmission. When the value of r_z is bigger, there is stronger and broader absorption between 0.336 and 0.585 μm, and there is only a slight difference between the two shapes. Overall, the transverse diameter of silver NPs is an important parameter that it determines the wavelength range of sunlight band absorption [20, 21], and r_z is related to the strength of the light absorption. In addition, spheroidal silver NPs have less light reflection and more transmission than hemispheroidal silver NPs especially when the wavelength is greater than 0.585 μm as shown in Fig. 3d, f.

Because of the better light trapping by silver NPs shown in Fig. 3, they can be used as antireflection coating to improve the light absorption of CS thin-film solar cells. As shown on the left side of Fig. 4, under $r_z/r_x = 1.0$, compared with Fig. 3a, b, the total light reflection is enhanced due to the presence of silicon surface; meanwhile, the total light absorption is also improved owing to the absorption of CS body. However, compared with the bare silicon shown in Fig. 4a, b, with the increase of hemispheroidal silver NP diameter, the antireflection and absorption are significantly improved when the ratio of D/P is greater than 0.5. However, for spheroidal silver NPs, in the majority absorption band of CS, there is strong light reflection effect which is bound to lead to the weakening of light absorption when the wavelength is longer than the transition wavelength (The transition wavelengths are 0.390 μm for $D/P = 0.3$, 0.430 μm for $D/P = 0.5$, and 0.485 μm for $D/P = 0.7$, respectively), and it can be used to explain why the silicon absorption enhancement is mainly in the shorter wavelengths mentioned in Xu et al.'s [9] study. In the same way, under $D/P = 1.0$, as shown on the right side of Fig. 4, the longitudinal diameter of silver NPs mainly affects the intensity of the light absorption, reflection, and transmission. For spheroidal NPs, there is also a transition wavelength for the different values of r_z (The transition wavelengths are 0.670 μm for $r_z/r_x = 0.5$, 0.730 μm for $r_z/r_x = 1.0$, and 0.800 μm for $r_z/r_x = 2.0$, respectively); when the wavelength is greater than the transitional wavelength, the light absorption and reflection properties become worse than bare CS. For hemispheroidal NPs, it seems

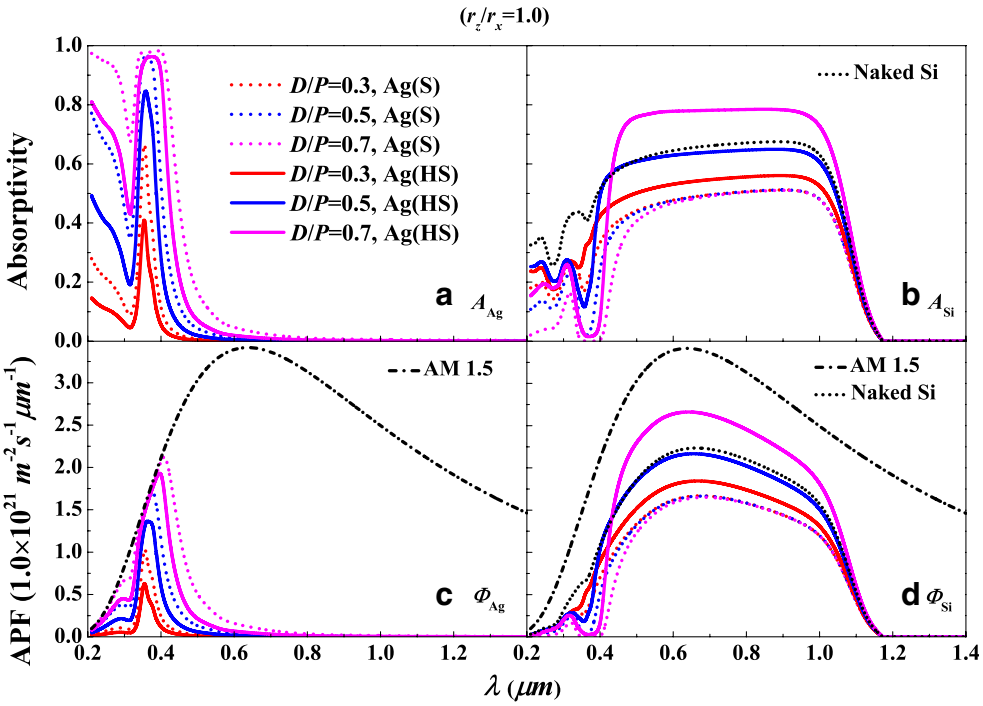

Fig. 5 Under $r_z/r_x = 1.0$, **a** and **c** are the light absorptivity A_{Ag} and absorptivity of photon flux (APF) Φ_{Ag} of silver NP coating, respectively; **b** and **d** are respectively the light absorptivity A_{Si} and APF Φ_{Si} of CS body compared to the bare silicon under AM. 1.5 spectrum

the bigger the longitudinal diameter, the better the optical properties. Moreover, the larger spheroidal NPs can enhance the absorption of infrared light as shown in Fig. 4e.

For the thin-film silicon solar cells, the two shapes of silver NPs result in completely different optical properties in the middle- and long-wave infrared regions. On the one hand, optical properties depend on the shapes and sizes of silver NPs, and on the other hand, the interface between hemispheroidal NPs and CS body is a flat surface, not a point contact, which greatly improves the path length and increases the light absorption in the CS body. Therefore, it can be concluded that hemispheroidal silver NPs as an antireflection coating can greatly enhance light absorption in thin-film silicon solar cells, and the larger the volume, the stronger the light absorption property as depicted in Fig. 4e. However, most of the light absorbed by silver NPs is used to generate heat and is hence a waste of light for thin-film solar cells. For this reason, the difference of light absorption distribution between the

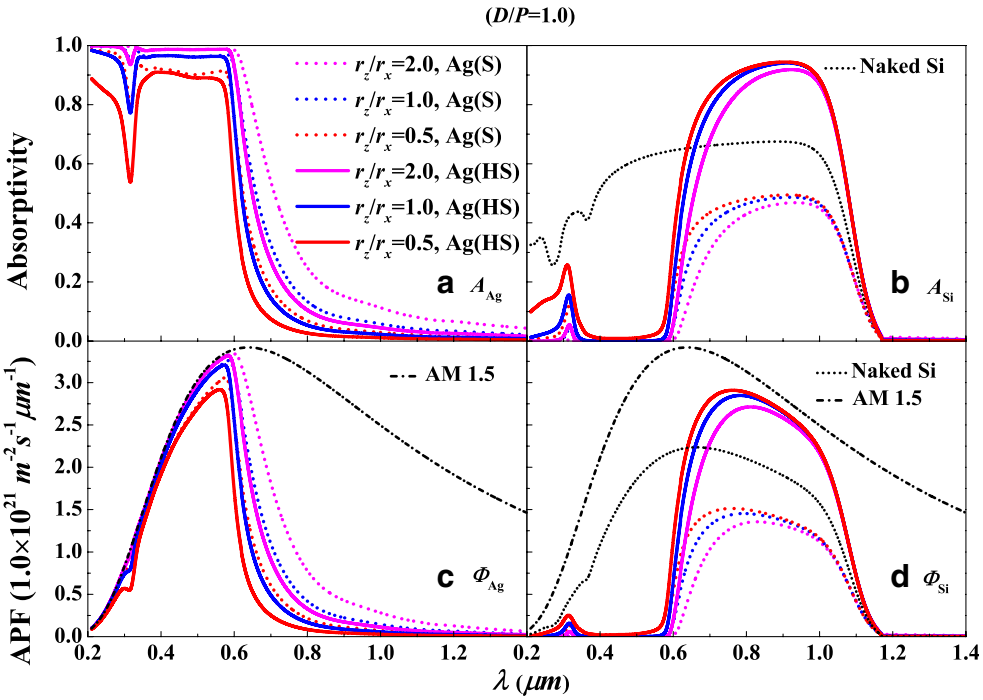

Fig. 6 Under $D/P = 1.0$, **a** and **c** are the light absorptivity A_{Ag} and absorptivity of photon flux (APF) Φ_{Ag} of silver NP coating, respectively; **b** and **d** are respectively the light absorptivity A_{Si} and APF Φ_{Si} of CS body compared to the bare silicon under AM. 1.5 spectrum

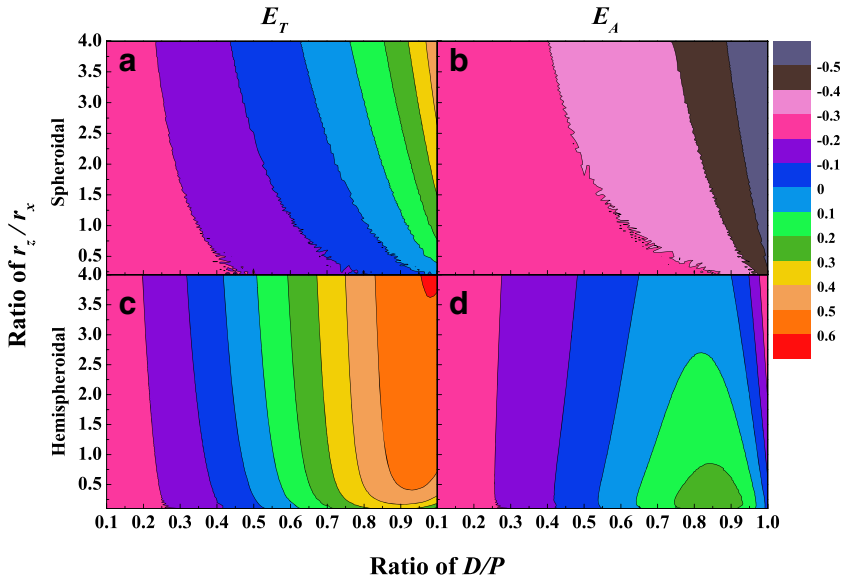

Fig. 7 **a**, **b**, **c**, and **d** are contour maps of enhancement factors E_T and E_A under different values of r_z/r_x and D/P, which correspond to the spheroidal and hemispheroidal silver NPs

silver NP antireflection layer and CS body should be further studied in order to obtain the appropriate parameters.

The total light absorption can be divided into two parts such that $A=A_{Ag}+A_{Si}$ as shown in Fig. 1a. The distribution of light absorption between them is calculated and shown in Figs. 5 and 6 under different parameters. Compared to silver NPs exposed in the air (Fig. 3b, e), silver NPs on the CS thin film show a subtle increase in the light absorption because of the multiple light reflection between the contact interfaces, as shown in Figs. 5a and 6a. With silver NPs as an antireflection coating, the larger the diameter of the NPs, the more the absorption of the middle- and long-wave infrared regions as seen on the left side of Fig. 6. But with CS body, in the region where the main light absorption and conversion take place, the absorption of medium and short waves decreases due to the intense absorption by silver NPs seen from the right side of Figs. 5 and 6. More importantly, for spheroidal silver NPs, there is no improvement in photon absorption in the CS body no matter how big the diameter or volume is. However, for hemispheroidal silver NPs, it is beneficial for efficiency of photon harvesting enhancement when with proper parameters.

Increasing the amount of photons which can be absorbed by CS body compared to the bare CS is what an antireflection coating does. To make the difference more intuitionistic between the silver NP coating and CS body, the three-dimensional illustration is shown in Fig. 7. As shown, two enhancement factors, namely efficient light trapping E_T and effective light absorption E_A, are used to quantitatively contrast the optical properties of the two shapes of silver NPs. For spheroidal NPs (Fig. 7a, b), E_T can reach more than 0.4, but E_A is negative and far less than zero. For hemispheroidal silver NPs, when the ratio of D/P approaches 1.0 and the ratio of r_z/r_x is greater than 4.0, E_T can reach more than 0.6. However, E_A has maximum value of about 0.26 when the ratio of D/P nears 0.86 and r_z/r_x approaches 0.22. In conclusion, Fig. 6 shows that spheroidal silver NPs are useless and not effective in improving the photon absorption of CS body. On the contrary, the hemispheroidal silver NPs, especially the flat hemispheroidal NPs, can greatly improve the light absorption of thin-film silicon solar cells, and this is in agreement with the similar results from other studies [7, 10, 22, 23]. Moreover, it is worth noting that in the optimum range, E_T is only about 0.40, not the biggest value 0.6, which means the pursuit of the best light trapping properties should take into consideration effective light absorption.

Conclusions

We have investigated the light trapping and the light absorption properties of two shapes (spheroidal and hemispheroidal) of silver NPs as antireflection coating for thin-film silicon solar cell. For the convenience of quantitative evaluation, two enhancement factors E_T and E_A are introduced, and the results show that spheroidal silver NPs are not suitable for use as antireflection coating due to their strong light absorption characteristics. However, the hemispheroidal silver NPs especially the flat NPs can be used for the enhancement of light transmission for silver NPs and increase light absorption for the thin-film silicon solar cells.

Acknowledgements This work was supported partially by the National High-tech R&D Program of China (2015AA034601), National Natural Science Foundation of China (91333122, 61204064, 51202067, 51372082, 51402106, and 11504107), Ph.D. Programs Foundation of Ministry of Education of China (20120036120006, 20130036110012), Par-Eu Scholars Program, and the Fundamental Research Funds for the Central Universities.

References

1. Pillai S, Green MA (2010) Plasmonics for photovoltaic applications. Sol Energy Mater Sol Cells 94:1481–1486
2. Spinelli P, Ferry VE, Groep JVD, Lare MV, Verschuuren MA, Schropp REI, Atwater HA, Polman A (2012) Plasmonic light trapping in thin-film si solar cells. J Opt 14(2):24002–24012
3. Tanabe K (2007) Optical radiation efficiencies of metal nanoparticles for optoelectronic applications. Mater Lett 61:4573–4575
4. Sekhon JS, Verma SS (2012) Rational selection of nanorod plasmons: material, size, and shape dependence mechanism for optical sensors. Plasmonics 7:453–459
5. Akimov YA, Koh WS (2011) Design of plasmonic nanoparticles for efficient subwavelength light trapping in thin-film solar cells. Plasmonics 6:155–161
6. Tang Y, Vlahovic B (2013) Metallic nano-particles for trapping light. Nanoscale Res Lett 8(1):65
7. Uhrenfeldt C, Villesen TF, Têtu A, Johansen B, Nylandsted Larsen A (2015) Broadband photocurrent enhancement and light-trapping in thin film Si solar cells with periodic Al nanoparticle arrays on the front. Opt Express 23:A525–A538
8. Cheng S, Wang X (2015) Efficient light trapping structures of thin film silicon solar cells based on silver nanoparticle arrays. Plasmonics 10(6):1–8
9. Xu Y, Xuan Y (2015) Design principle for absorption enhancement with nanoparticles in thin-film silicon solar cells. J Nanopart Res 17(7):1–12
10. Catchpole KR, Polman A (2008) Design principles for particle plasmon enhanced solar cells. Appl Phys Lett 93:191113
11. Starowicz Z, Kulesza-Matlak G, Lipiński M (2015) Optimization studies on enhanced absorption in thin silicon solar cell by plasmonic silver nanoparticles for the front side configuration. Plasmonics 10(6):1639–1647
12. Kasten F, Young AT (1989) Revised optical air mass tables and approximation formula. Appl Opt 28:4735–4738
13. Duan Z, Li M, Mwenya T, Pengfei F, Li Y, Song D (2016) Effective light absorption and its enhancement factor for silicon nanowire-based solar cell. Appl Opt 55:117–121
14. Santbergen R, Smets AHM, Zeman M (2013) Optical model for multilayer structures with coherent, partly coherent and incoherent layers. Opt Express 21:A262–A267
15. Santbergen R, van Zolingen RJC (2008) The absorption factor of crystalline silicon PV cells: a numerical and experimental study. Sol Energy Mater Sol Cells 92(4):432–444
16. Cai W, Shalaev V (2010) Optical metamaterials: fundamentals and applications. Springer, New York, pp p29–p30
17. Palik E D (1985) Handbook of optical constants of solids, Vol. 1. Academic Press 189:p350, p547
18. Liu W, Wang X, Li Y, Geng Z, Yang F, Li J (2011) Surface plasmon enhanced GaAs thin film solar cells. Sol Energy Mater Sol Cells 95(2):693–698
19. In S, Mason DR, Lee H, Jung M, Lee C, Parkl N (2015) Enhanced light trapping and power conversion efficiency in ultrathin plasmonic organic solar cells: a coupled optical-electrical multiphysics study on the effect of nanoparticle geometry. ACS Photonics 2:78–85
20. Cheng S, Jie S, Wang X (2015) A Design of Thin Film Silicon Solar Cells Based on silver nanoparticle arrays. Plasmonics 10:633–641
21. Akimov YA, Ostrikov K, Li EP (2009) Surface plasmon enhancement of optical absorption in thin-film silicon solar cells. Plasmonics 4:107–113
22. Alemu N, Chen F (2014) Plasmon-enhanced light absorption of thin-film solar cells using hemispherical nanoparticles. Phys Status Solidi A 211(1):213–218
23. Temple TL, Mahanama GDK, Reehal HS, Bagnall DM (2009) Influence of localized surface plasmon excitation in silver nanoparticles on the performance of silicon solar cells. Sol Energy Mater Sol Cells 93(11):1978–1985